scientific reports

Check for updates

OPEN

GRAF1 deficiency leads to defective brown adipose tissue differentiation and thermogenic response

Xue Bai[1,4], Qiang Zhu[1,4], Matthew Combs[1], Martin Wabitsch[2], Christopher P. Mack[1,3] & Joan M. Taylor[1,3]✉

Adipose tissue, which is crucial for the regulation of energy within the body, contains both white and brown adipocytes. White adipose tissue (WAT) primarily stores energy, while brown adipose tissue (BAT) plays a critical role in energy dissipation as heat, offering potential for therapies aimed at enhancing metabolic health. Regulation of the RhoA/ROCK pathway is crucial for appropriate specification, differentiation and maturation of both white and brown adipocytes. However, our knowledge of how this pathway is controlled within specific adipose depots remains unclear, and to date a RhoA regulator that selectively controls adipocyte browning has not been identified. Our study shows that GRAF1, a RhoGAP, is highly expressed in metabolically active tissues, and closely correlates with brown adipocyte differentiation in culture and in vivo. Mice with either global or adipocyte-specific GRAF1 deficiency exhibit impaired BAT maturation and compromised cold-induced thermogenesis. Moreover, defects in differentiation of human GRAF1-deficient brown preadipocytes can be rescued by treatment with a Rho kinase inhibitor. Collectively, these studies indicate that GRAF1 can selectively induce brown adipocyte differentiation and suggest that manipulating GRAF1 activity may hold promise for the future treatment of diseases related to metabolic dysfunction.

Keywords GRAF1, Adipose tissue, Browning, Thermogenesis, Energy metabolism

Adipose tissue is comprised of two major cell types- white and brown adipocytes- that have opposing energetic functions. White adipocytes primarily function to store excess lipid and an over-abundance of white adipose tissue (WAT) leads to unfavorable outcomes due to disruption in many metabolic and hormonal activities. In contrast, brown adipocytes consume glucose and lipid and brown adipose tissue (BAT) dissipates energy through uncoupled oxidative phosphorylation-induced heat generation, a process necessary for thermoregulation in small animals and infants. As obesity results from a disparity between energy intake and expenditure, the identification of new molecules and signals that can drive fat browning may lead to attractive targets for the treatment of obesity and related cardiometabolic disorders.

WAT and BAT are located in discrete depots that are distributed throughout the body and are derived from a diverse group of progenitor cells. While we do not yet know the precise origins of cells within each of these tissues, current lineage tracing studies indicate that Myf5-expressing progenitor cells that originate in the dermomyotome give rise to greater than 90% of inter- and sub-scapular BAT (iBAT and sBAT) which are the largest BAT depots in mice[1,2]. Other adipose depots likely arise from a more heterogeneous population of progenitors. For example, the contribution of Myf5 progenitors to WAT varies tremendously (from 5 to 60%) based on anatomic locale and sex[1]. The mural cell compartment of the vasculature also appears to be a major contributing source of adipogenic precursors in various WAT compartments.

Despite their heterogeneous origins, white and brown adipogenic precursors share some common transcriptional programs. For example, peroxisome proliferator–activated receptor gamma (PPARγ) is a master regulator of adipocyte differentiation and this transcription factor drives expression of a number of genes common to all adipocytes including adiponectin and fatty acid binding protein 4 (FABP4)[3,4]. Moreover, classical

[1]Department of Pathology and Laboratory Medicine, University of North Carolina, Chapel Hill, NC 27599, USA. [2]Department of Pediatrics and Adolescent Medicine, Ulm University Medical Center, 89075 Ulm, Germany. [3]McAllister Heart Institute, University of North Carolina, 160 North Medical Drive, 501 Brinkhous-Bullitt, CB# 7525, Chapel Hill, NC 27599, USA. [4]These authors contributed equally: Xue Bai and Qiang Zhu. ✉email: joan_m_taylor@med.unc.edu

brown adipocytes that originate from the dermomyotome and beige adipocytes that are intermingled in WAT depots share PGC1α- and PRDM16- dependent transcriptional programs that drive mitochondrial biogenesis and induce a common subset of BAT-selective genes. These include, among others, Cidea which promotes lipolysis and lipogenesis and uncoupling protein 1 (UCP-1) which is responsible for facilitating thermogenesis through uncoupled respiration[5].

Importantly, both white and brown adipocytes undergo dynamic and reversible phenotypic conversions in response to environmental cues. For example, thermoneutrality or exposure to high fat diet can induce BAT to undergo reversible WAT-like remodeling. Conversely, long-term cold exposure, agonist-induced activation of the β3 adrenergic pathway, or physical activity can promote certain WAT depots to undergo browning. The beneficial physical activity-induced phenotypic changes are mediated, at least in part, by skeletal-muscle derived factors including fibroblast growth factors(FGFs) and bone morphogenic proteins (BMPs)[6,7].

BMP 4, 6, and 7 are particularly strong inducers of brown and beige adipogenesis and, while we do not fully understand the underlying signaling mechanisms, downregulation of RhoA-mediated signaling has been shown to be important[8–12]. For example, down-regulation of RhoA in white adipocytes promotes beige cell development and heterozygous germline depletion of the RhoA-dependent kinase, ROCK2, or treatment with Rho kinase inhibitors promoted WAT browning and led to protection from diet-induced obesity and insulin resistance in mice[13]. Interestingly, the dynamic regulation of RhoA is also important to control the fate of mesenchymal stem cells and multi-potent progenitors wherein low RhoA activity favors pre-adipocyte specification while high RhoA activity promotes specification towards osteoblast, smooth- or skeletal muscle cell fates[14]. Mechanistically, RhoA/ROCK signaling promotes these cell fate conversions by modulating both actin cytoskeleton-dependent shape changes and altering gene transcription (RhoA activity inhibits the pro-adipogenic transcription factor, PPARγ and activates myogenic SRF/MRTFA- mediated gene transcription)[15,16].

RhoA, like all small GTPases, cycles between an inactive GDP-bound form and an active GTP-bound form and its activity is enhanced by guanine nucleotide exchange factors (GEFs) and inhibited by GTPase-activating proteins (GAPs). To date, two RhoA-specific GAPs have been identified as critical regulators of adipogenesis, p190B and DLC1. P190B limits RhoA activity in myogenic precursors and is necessary for these cells to adopt a pre-adipocyte fate[17–19]. On the other hand, DLC1 limits RhoA activity in pre-adipocytes and functions to promote white and brown adipogenesis[20]. However, a GAP that selectively controls adipocyte browning has not yet been identified. Herein, we show that the multidomain containing RhoA-GAP termed GRAF1 (guanosine triphosphatase (GTPase) regulator associated with FAK-1, also named Arhgap26)[21,22]that was previously reported to be strongly expressed in highly metabolic tissues (including heart, brain, and skeletal muscle) is also strongly expressed in BAT and functions to selectively promote the differentiation and activation of BAT. Our findings highlight the possibility that GRAF1 could be a new therapeutic target to combat obesity and associated morbidity.

Results

GRAF1 expression correlates with BAT maturation in mouse and human cells

We previously reported that GRAF1 was transiently upregulated during skeletal muscle development (E17-P4) and again following adult muscle injury and that, in these contexts, GRAF1 promoted myoblast differentiation by limiting RhoA activity[23]. Interestingly, while dissecting various muscles from adult GRAF1 hypomorphic ($GRAF1^{gt/gt}$) mice, we noticed that their iBAT depots were relatively pale compared to WT controls. Since myocytes and BAT share common Myf5-expressing precursors[1,18,24,25] and both cell types require RhoA inactivation for differentiation and maturation[26,27], we further investigated a possible role for GRAF1 in BAT development.

In mice, iBAT and sBAT depots develop during late embryogenesis, and, upon expression profiling in juvenile mice (3 weeks postnatal), we found that GRAF1 was highly expressed in these major BAT depots. GRAF1 was also expressed (albeit at a lower level) in subcutaneous WAT (scWAT) (Fig. 1a). Interestingly, GRAF1 mRNA levels in iBAT increased nearly 20-fold from 1 week to 3 months of age (Fig. 1b) and this increase paralleled the expression of BAT maturation genes including PPARγ, the thermogenic protein UCP1, and the mitochondrial marker ND5. In contrast, GRAF1 levels did not significantly change during scWAT maturation (Fig. 1b) and preliminary analysis of GRAF1 mRNA in the visceral WAT compartment in adult mice was low, comparable to the levels observed in scWAT from 3-month-old mice (data not shown).

We noticed two GRAF1 immuno-reactive bands in Western analyses of immature sBAT and iBAT and that the immune-reactive band for scWAT appeared to exhibit a slower mobility (Fig. 1a). Likewise, while only one GRAF1 immune-reactive band was observed in adult scWAT and iBAT tissue, GRAF1 in adult scWAT also exhibited a slower mobility than GRAF1 in adult iBAT (Figure S1a). Given that we previously reported that phosphorylation of Ser and Thr residues within the serine/proline-rich region of GRAF1 induced an upward mobility shift on SDS-PAGE[28], we next tested the extent to which GRAF1 phosphorylation might account for the slower migrating form observed in scWAT. As shown in figure S1a, treatment with calf intestinal phosphatase (CIP) failed to alter the mobility of GRAF1 in either depot. Thus, the distinctions observed in the mobility of GRAF1 between scWAT and iBAT could arise from additional post-translational modifications or alternative splicing mechanisms.

We next used cultured cell models to confirm and extend the idea that GRAF1 is robustly induced during brown adipocyte differentiation. First, using WT-1 cells (a validated in vitro model of brown adipogenesis)[29], we found that GRAF1 expression was dynamically and transiently increased at the onset of differentiation (Fig. 1c, d) and that its induction occurred prior to, or concomitant with, expression of BAT marker genes UCP1, PPARγ, and ND5 (Fig. 1d). This finding is consistent with prior reports indicating that RhoA/ROCK signaling is down-regulated upon the induction of adipocyte differentiation in these cells. A similar dramatic increase in GRAF1 expression was observed in human preadipocytes (Simpson-Golabi-Behmel syndrome, SGBS)

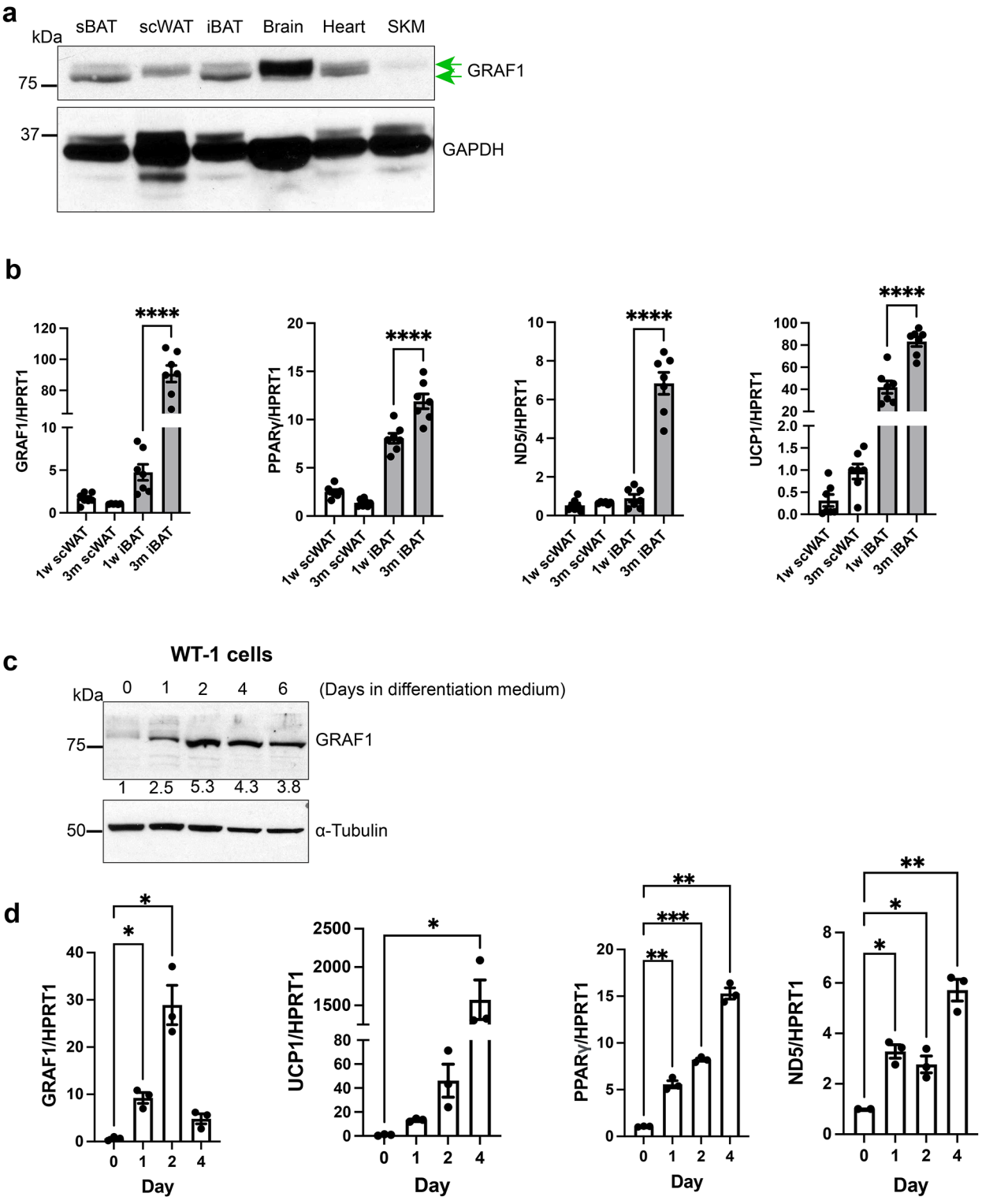

Fig. 1. GRAF1 expression closely correlates with BAT maturation. (**a**) GRAF1 protein levels in 3-week postnatal male mouse tissue detected by Western blotting. scWAT, sub-cutaneous white adipose tissue; iBAT and sBAT, inter- and sub-scapular brown adipose tissue, SKM, skeletal muscle. Two green arrows denote the presence of two GRAF1 bands observed in the blot. (**b**) qRT-PCR of GRAF1 and adipocyte marker genes in indicated adipose depot isolated from 1 week old and 3-month-old male and female mice, n=6-7. (**c**,**d**) WT-1 pre-brown adipocytes were exposed to brown fat-inducing insulin differentiation medium for the indicated times, subsequent Western blotting analysis of GRAF1 level ((**c**) densitometric values of GRAF1 were measured and presented below each corresponding GRAF1 band, blot is representative of n=3 independent experiments) or qRT-PCR analysis of indicated adipocyte markers ((**d**) n=3 biological replicates). Data are represented as mean ± SEM, *P < 0.05; **P < 0.01; ***<0.001;****P < 0.0001 by two-tailed student's t-test (**b**) or mixed effect analysis with post-hoc Fisher's LSD test (**d**).

following exposure to brown adipocyte differentiation medium (Figure S1b, top panel). Note that adipogenic differentiation of these cells was accompanied by lipid droplet accumulation and characteristic brown phenotype observed using light microscopy (Fig S1b, bottom panel). Likewise, GRAF1 protein was markedly induced following treatment of mouse 3T3-L1 adipocytes with a BAT induction cocktail (Figure S1c). Collectively, these studies indicate that GRAF1 might play an important and conserved role in promoting BAT development.

GRAF1 is necessary for BAT maturation and thermogenesis

We next compared BAT and WAT marker gene expression in tissue isolated from WT mice or from global GRAF1-deficient mice (GRAF1$^{gt/gt}$) which harbors the gene trapping vector VICTR48 within the first intron of Graf1. These mice lines are viable and fertile with no obvious abnormalities under baseline conditions[30]. As shown in Fig. 2a, we found no differences in expression of UCP1, PPARγ or ND5 in scWAT or iBAT isolated

◀**Fig. 2**. GRAF1 does not alter adipocyte specification but is required for brown fat formation and function. (**a**) iBAT and scWAT isolated from 1 week old male and female WT and GRAF1$^{gt/gt}$ mice exhibited similar levels in adipose marker gene expression as assessed by qRT-PCR ($n=6$–9/group), indicating that GRAF1 is not necessary for white or brown adipose tissue specification. The expression of the target gene is compared relative to its expression in WT scWAT. (**b**) iBAT isolated from 2–3-month-old male and female GRAF1$^{gt/gt}$ mice exhibited significantly lower levels of brown fat marker genes that mediate thermogenesis compared to littermate control mice as assessed by qRT-PCR ($n=7$/group). (**c**) Representative H&E stain of iBAT isolated from 2–3-month-old GRAF1$^{gt/gt}$ and WT mice. Note the transition from multilocular adipocytes to a unilocular white-like adipocyte phenotype, indicative of BAT whitening in GRAF1$^{gt/gt}$ iBAT depot, ($n=5$/group). scale bar: 60 µm. (**d**) Quantification of lipid area (normalized to the number of nuclei) in iBAT shown in (**c**,**e**). Target genes in scWAT isolated from 2–3-month-old male and female GRAF1$^{gt/gt}$ mice were assessed by qRT-PCR. ($n=7$/group). **f**. Female GRAF1$^{gt/gt}$ and WT mice were housed at sub-thermoneutral temperatures (22 °C) and subjected to overnight fasting followed by an acute bout of cold stress (7 °C) and their body temperatures were measured over time using a rectal thermometer($n=9$ WT, $n=7$ GRAF1$^{gt/gt}$). **g.** Representative UCP1 DAB stain of iBAT isolated from cold exposed 2–3-month-old female GRAF1$^{gt/gt}$ and WT mice.Scale bar: 25 µm. Quantitative analysis of images using Fiji revealed a significant reduction in % positivity of UCP1 staining (61.0% +/− 25.2% for WT ($n=3$) and 2.8% +/− 1.4% for GRAF1$^{gt/gt}$ ($n=4$); $p<0.05$). (**h**,**i**) serum lactate level were measured in fed female mice at basal condition ((**h**) $n=6$/group) or from cold exposure (**i**). Data are represented as mean ± SEM, ns, not significant; $^{*}P<0.05$; $^{**}P<0.01$; $^{***}<0.001$;$^{****}P<0.0001$ by two-tailed student's t-test(**a**,**b**, **d**,**e**, **h**,**i**) or repeated measures ANOVA with post-hoc Fisher's LSD test (**f**).

from 1 week old WT and GRAF1$^{gt/gt}$ mice, suggesting that GRAF1 does not play an important role in adipose tissue specialization. However, since adipose tissue maturation happens gradually after birth through young adulthood[31–33] and GRAF1 expression was robustly increased during this timeframe, we reasoned that GRAF1 might impact adipose differentiation/maturation. Indeed, as shown in Fig. 2b, iBAT depots isolated from 2 to 3 month-old GRAF1-deficient mice exhibited a dramatic reduction in BAT marker gene expression relative to littermate control WT mice. For example, BAT thermogenesis genes (UCP1, Elovl3), mitochondrial genes (ND5, COX7a), and PPARγ, the master regulator gene of adipocyte differentiation were all significantly reduced, indicating a differentiation/maturation defect in the iBAT of GRAF1 hypomorphs. Accordingly, H&E staining of iBAT from 2 to 3 month old GRAF$^{gt/gt}$ mice revealed a "white like" appearance as demonstrated by a substantial increase in lipid deposition and enlarged lipid droplets compared to iBAT from littermate WT control mice(Fig. 2c, d). scWAT from 2 to 3 month old GRAF1-deficient mice also exhibited a significant down-regulation of brown marker genes including UCP1 and Elovl3 but not of the general adipose marker adiponectin, which was significantly increased (Fig. 2e). These data indicate that GRAF1 differentially impacts WAT and BAT maturation. Despite these changes, and consistent with our prior report, there was no difference in the body weights of GRAF1$^{gt/gt}$ mice and littermate control mice fed ad libitum[30]. This finding is consistent with other mouse models that exhibit defects in brown adipose development, yet do not develop obesity, such as those with the loss of the uncoupling protein UCP-1[34], or the fatty acid metabolism gene Adipose acyl-CoA synthetase-1[35].

To determine the impact of GRAF1-dependent changes in BAT differentiation on BAT function, we next exposed mice housed at sub-thermoneutral temperatures to overnight fasting followed by an acute bout of cold stress (~7 °C) and measured their body temperatures over time. As shown in Fig. 2f, GRAF1-deficient mice exhibited a remarkable reduction in thermogenic capacity under these conditions. Accordingly, iBAT from cold exposed GRAF1$^{gt/gt}$ mice exhibited a significantly reduced UCP1 protein levels relative to cold exposed WT mice as assessed by IHC (Fig. 2g, S1d). Moreover, cold-exposed, fed GRAF1$^{gt/gt}$ mice exhibited a significant reduction in serum lactate levels, while their baseline lactate levels were unaffected (Fig. 2h, i). Since circulating lactate is the main fuel that drives the tricarboxylic acid cycle (TCA cycle) in a fasted state[36], the decreased lactate might suggest enhanced TCA cycling due to beta-oxidation defects in GRAF1$^{gt/gt}$ mice. Nonetheless, given our knowledge regarding GRAF1's role in skeletal muscle maturation, we realized that the drop in temperature coupled with the reduced lactate production observed in GRAF1$^{gt/gt}$ mice could be due (at least in part) to a reduced capacity for shivering thermogenesis in these germline-deficient mice. To begin to distinguish between these two possibilities, we first sought to determine if GRAF1 can act in a cell autonomous fashion to promote BAT maturation. To this end, we turned to primary pre-brown adipocyte cultures isolated from the stromal vascular fraction (SVF) of iBAT as these cells have been reported to faithfully recapitulate brown adipocyte maturation when exposed to serum-containing media supplemented with insulin, triiodothyronine (T_3), dexamethasone, IBMX and rosiglitazone[37]. Importantly, upon induction with differentiation media, SVF cells transfected with GRAF1 siRNA exhibited a significant reduction in browning capacity compared to control siRNA treated cells as assessed by UCP1 expression and oil red O staining (Fig. 3a–c). These findings indicate that GRAF1 levels can directly impact the differentiation of brown adipocytes.

Next, to further explore an adipocyte-autonomous role for GRAF1 in BAT formation and function, we developed a new mouse model using targeting vectors from Eucomm to conditionally target the GRAF1 allele (Fig S2 a and b) and crossed GRAF1$^{fl/fl}$ mice with Adipoq Cre mice[38] to establish an adipose-specific GRAF1 knockout mouse line (GRAF1^{AKO}) that led to a significant depletion of GRAF1 in BAT and scWAT (Fig. 3d). Importantly, while not as dramatic as observed in the GRAF1$^{gt/gt}$ mice, the thermogenic capacity of GRAF1^{AKO} mice was significantly blunted when compared to genetic control mice (Fig. 3e). Also, the thermogenic gene expression profile in mature iBAT was significantly reduced in cold-exposed GRAF1^{AKO} mice when compared to similarly-treated genetic control mice (Fig. 3f). Consistent with the more modest impact on thermogenesis,

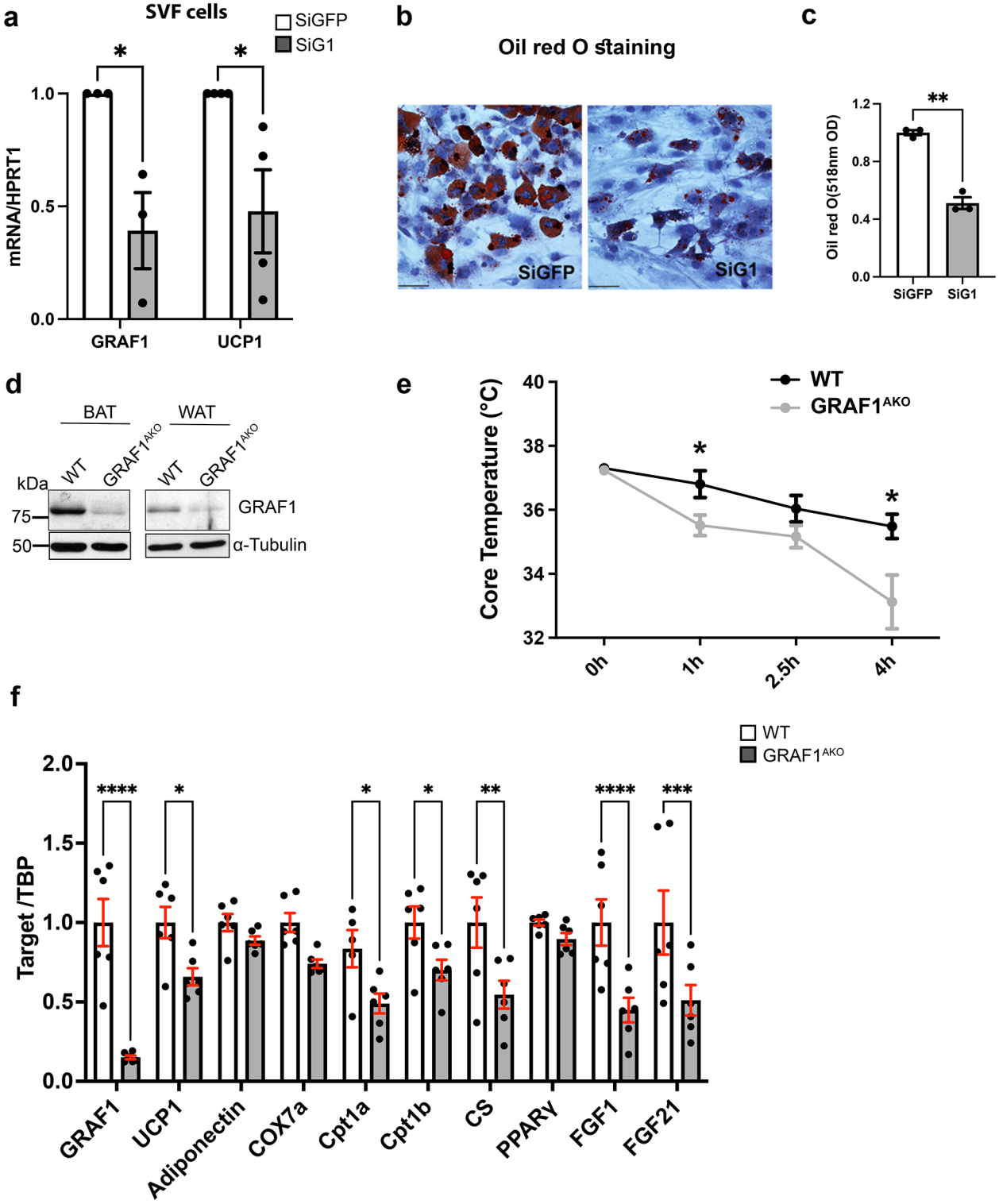

Fig. 3. Adipocyte-autonomous role for GRAF1 in BAT formation and function. (**a**) differentiation of primary pre-brown adipocytes isolated from the stromal vascular fraction (SVF) of iBAT was reduced by GRAF1 depletion as assessed by UCP1 expression. $n = 3$–4. (**b**,**c**). Oil red O staining of differentiated SVF cells treated with indicated siRNA (**b**) and quantification of oil red O staining (**c**). (siG1 denotes siGRAF1). $n = 3$/treatment. (**d**) Assessment of GRAF1 depletion in BAT and scWAT in female WT and GRAF1^{AKO} mice via Western blot analysis. **e**. Female GRAF1^{AKO} mice exhibited cold intolerance when subjected to conditions described in (Fig. 2f). $n = 5$–6/group. (**f**) qRT-PCR data showed significantly decreased markers of brown adipogenesis, mitochondrial components and FGFs in iBAT of GRAF1^{AKO} mice. $n = 6$/group. Data are represented as mean ± SEM, $^{*}P < 0.05$; $^{**}P < 0.01$; $^{***}<0.001$;$^{****}P < 0.0001$ by two-tailed student's t-test (**a**, **c**,**f**) or repeated measures ANOVA with post-hoc Fisher's LSD test (**e**).

while iBAT from GRAF1^{AKO} mice exhibited a significant reduction in UCP1 expression, the decrease was not as robust as observed in GRAF1$^{gt/gt}$ mice (possibly due to incomplete recombination in our model). Nonetheless, GRAF1^{AKO} iBAT also exhibited significantly reduced expression of the mitochondrial genes Cpt1a, Cpt1b and CS. In addition, GRAF1^{AKO} iBAT also exhibited significant reductions in the expression of growth factors known to promote glucose homeostasis including FGF1, which acts in an autocrine fashion to promote glucose uptake in activated BAT and FGF21, an endocrine factor that has been linked to the cardiometabolic benefits of brown fat activation through its ability to promote glucose homeostasis in BAT, skeletal muscle, liver and brain. Collectively, these data confirm that GRAF1 plays an important, adipocyte-autonomous role in BAT formation and function.

GRAF1 promotes brown phenotypes by limiting RhoA/ROCK signaling

We next turned to the use of cultured brown adipocytes to confirm and extend these findings. In support of a cell autonomous role for GRAF1 to promote brown adipocyte differentiation and function, we found that siRNA mediated GRAF1 depletion significantly attenuated UCP1 protein levels in WT-1 brown adipocytes exposed to differentiation medium (DM; Fig. 4a, b). Because previous studies have shown that the downregulation of RhoA-ROCK signaling is necessary and sufficient to promote adipogenesis, we reasoned that GRAF1 might promote BAT differentiation by controlling this pathway. To test this possibility, we quantified RhoA activity in brown adipocytes using a standard GST-rhotekin precipitation assay. As shown in Fig. 4c and d, GRAF1-depleted WT-1 cells exhibited significantly higher levels of RhoA activity in comparison with control siRNA-treated cells following treatment with the RhoA agonist, sphingosine-1-phosphate(S1P). Importantly, UCP-1 expression was also significantly reduced in GRAF1-depleted SGBS human brown adipocyte cells and this response was reversed by co-treatment with the ROCK inhibitor, Y27632 (Fig. 4e and Fig S2c). Collectively, these data support the likelihood that GRAF1 promotes brown adipocyte differentiation by limiting RhoA/ROCK signaling.

Discussion

Adipose tissue in mammals is a vital component of the energy regulation system and consists of two primary types: white adipocytes and brown adipocytes. White adipocytes are characterized by their large central lipid droplets, serving as reservoirs for storing excess energy in the form of triglycerides. In contrast, brown adipocytes feature small lipid droplets and a high number of mitochondria, enabling them to dissipate energy as heat through a process known as thermogenesis[39,40]. The discovery of metabolically active brown adipose tissue (BAT) in healthy adult humans and beige adipocytes within subcutaneous white adipose tissues (scWAT) has generated significant interest in the biology of brown and beige adipocytes due to their unique ability to improve whole-body glucose and lipid metabolism by consuming substantial amounts of blood glucose and lipids. Consequently, identifying molecules and signals that can regulate brown fat differentiation and function has become an attractive target for potential treatments of obesity and diabetes. Our study demonstrates for the first time that GRAF1 regulates brown adipogenesis. Depletion of GRAF1 reduces brown adipocyte differentiation and thermogenesis function in vivo, highlighting its unique role in mediating BAT cell fate.

The differentiation, activation, and maintenance of brown and beige adipocytes are governed by a complex interplay of multiple factors. These factors include endocrine signals such as fibroblast growth factors(FGFs) and bone morphogenic protein factors(BMPs), as well as critical transcription factors like PRDM16, PGC1α, PPARγ, and Foxp1[6,7,41–43]. Of particular interest, the RhoA/ROCK pathway has emerged as a key player in regulating adipogenesis. Previous studies have shown that disrupting this pathway, either through the expression of dominant-negative RhoA or the inhibition of ROCK, promotes differentiation in various adipogenic cell types, highlighting the significance of this pathway. Mechanistically, induction of adipocyte differentiation leads to downregulation of RhoA-ROCK signaling, which promotes disassembly of F-actin stress fibers and results in marked changes in cell shape that are thought to be important for lipid droplet accumulation. Depolymerization of F-actin also leads to accumulation of monomeric G-actin, which binds and sequester MRTFs in the cytosol, preventing their nuclear translocation. As MRTFs and their co-factor, SRF repress PPARγ, this critical step allows for the expression of PPARγ and its target genes, facilitating the development and maintenance of adipocyte characteristics during adipogenic differentiation[15,16,44].

The Rho GTPase can exist in either an inactive GDP-bound or an active GTP-bound form and is modulated by guanine nucleotide exchange factors (GEFs) and GTPase-activating proteins (GAPs)[45].The comprehensive understanding of the diverse regulators of Rho GTPase/ROCK in adipose tissues and their in vivo functional consequences remains relatively unexplored. Our previous studies have shown that GRAF1 is a bona fide RhoGAP and plays important roles in processes like myoblast fusion, which require GAP-dependent actin remodeling[30]. Given GRAF1's established function as a RhoGAP in various tissues, we hypothesized that it might also play a pivotal role in modulating RhoA activity during adipogenesis. Indeed, we observed that GRAF1 is highly and selectively expressed in metabolically active tissues, including brown adipose tissue (BAT), brain, and heart, and its expression profile closely correlated with brown adipocyte differentiation. This association is evidenced by the upregulation of GRAF1 in response to brown adipocyte differentiation medium in various cultured adipocytes and the significant increase in GRAF1 mRNA levels during the maturation stage of BAT in mice, but much less so in WAT. GRAF1 deficiency, as observed in primary pre-brown adipocyte cultures and in both global and adipose-specific GRAF1-deficient mice, significantly blunted brown adipose differentiation in a RhoA/Rho kinase dependent fashion. Furthermore, cold-challenged GRAF1-deficient mice exhibited an inability to efficiently regulate thermogenesis and exhibit lower levels of UCP1 expression. These data are consistent with a previous report that selective activation of RhoA in brown adipocytes (engendered by UCP1-driven Gq overexpression) reduces UCP1 expression and reduces O_2 consumption following cold exposure[46]. Collectively, these studies suggest that limiting RhoA activation is important for both BAT maturation and function and that GRAF1 plays a key role in this process.

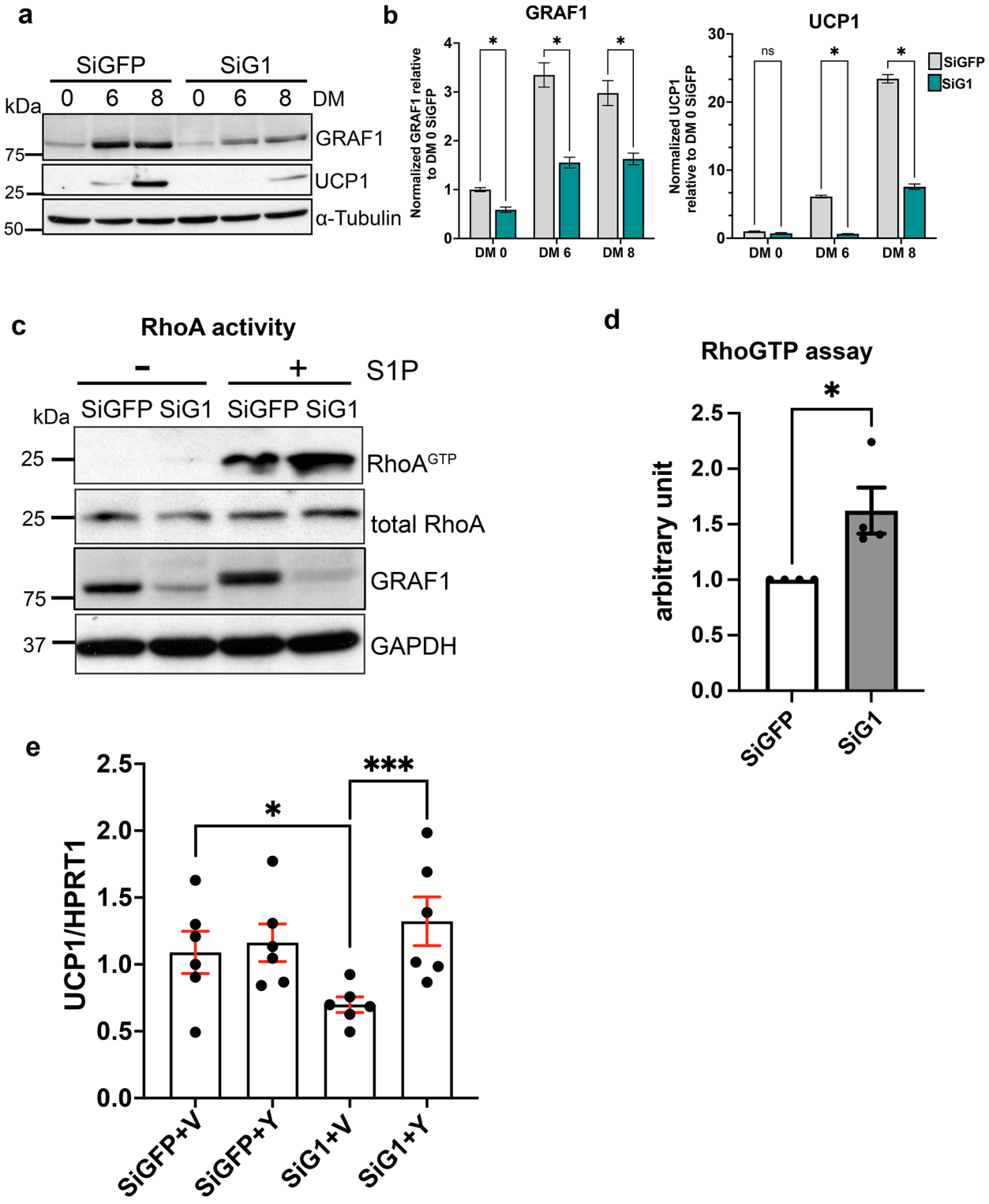

Fig. 4. GRAF1 promotes BAT differentiation by limiting RhoA/ROCK signaling. (**a**,**b**) 24 h following siRNA transfection, WT-1 pre-brown adipocytes were induced to differentiate into brown adipocytes over the indicated days using specific induction and differentiation factors (DM). Brown adipocyte differentiation was assessed by measuring UCP1 levels via Western blot (**a**) and quantified through densitometry(**b**). (**c**,**d**) RhoA activity in siRNA transfected WT-1 brown adipocytes was assessed by a standard GST-rhotekin precipitation assay(**c**) and quantified(**d**), $n = 4$ independent experiments. S1P denotes sphingosine-1-phosphate. (**e**) ROCK inhibitor Y27632 restored UCP-1 expression in GRAF1-depleted SGBS human brown adipocytes($n = 6$/group). The cells were transfected with specified siRNA for 24 h and subsequently treated with either Vehicle(V) or the ROCK inhibitor Y27632(Y) during the brown adipocyte differentiation. siG1 refers to siGRAF1. Data are represented as mean ± SEM, *ns* not significant; $^{*}P < 0.05$; $^{**}P < 0.01$; ***<0.001 by two-tailed student's t-test (**b**,**d**) or two-way ANOVA with post-hoc Fisher's LSD test (**e**).

Our mechanistic studies showed that GRAF1 depletion in a brown preadipocyte cell line increased Rho activity, suggesting that GRAF1 mediates brown adipocyte differentiation by GAP-dependent Rho GTPase inhibition. Interestingly, GRAF1 also possesses BAR (Bin/amphiphysin/Rvs) and PH (pleckstrin homology) domains that are involved in sensing and inducing membrane curvature and determining membrane binding specificity. Interestingly, these domains in combination with an isoform-specific hydrophobic segment (found in brain-selective GRAF1a) were previously reported to drive GRAF1a association with lipid droplets, an event that promoted lipid droplet clustering and reduced lipolysis[47,48]. While our current study focused on mouse GRAF1.2 (the ortholog of GRAF1b in humans) which does not contain this hydrophobic region, future studies are warranted to determine the extent to which GRAF1.2/GRAF1b may regulate adipocyte lipid droplet homeostasis.

There are a few notable limitations of our studies. Firstly, while we showed that GRAF1 similarly impacts BAT maturation in both male and female mice, our functional studies were only performed on female mice. Thus future studies in male mice will be necessary to determine the applicability of these findings to both sexes. Secondly, it is formally possible that additional mechanisms beyond BAT maturation underlie the thermogenic defects observed in GRAF1$^{gt/gt}$ and GRAF1^{AKO} mice. Indeed, the fact that GRAF1$^{gt/gt}$ mice in this study appeared to be even more cold-intolerant than GRAF1^{AKO} mice raises the intriguing possibility that GRAF1 might play an additional role in non-adipose thermogenesis. In this regard, given that we previously reported that GRAF1 promotes skeletal muscle differentiation and fusion[23], future studies are necessary to determine the extent to which shivering-induced thermogenesis or a skeletal muscle to adipose signaling axis might be involved[49]. With respect to GRAF1 dependent thermogenic defects in GRAF1^{AKO} mice, it will be of future importance to explore the possibility that changes in WAT function are also involved (i.e. WAT browning and/or WAT-dependent mobilization of factors necessary for shivering induced thermogenesis). Moreover, it will be of future interest to analyze protein levels of relevant WAT and BAT markers and mass of WAT and BAT depots of GRAF1^{AKO} and WT mice over time and/or following treatment with a high fat diet in order to confirm and extend the possibility that GRAF1 plays a major role in brown but not white adipogenesis. It will also be of future interest to explore the possibility that GRAF1 impacts WAT beiging and that this function could play an additive role in thermogenesis. Moreover, while our studies show a clear link between GRAF1 and production of the major thermoregulator, UCP1, in BAT, future studies will be required to determine a definitive role for GRAF1 in regulating mitochondrial function. Notably, our recent studies uncovered a novel role for GRAF1 in maintaining mitochondrial quality control in cardiomyocytes[28] and it will be of future interest to determine the extent to which this GRAF1-dependent process controls O_2 consumption in various adipose depots.

Previous studies have demonstrated that p-190 B is a RhoGAP can that shift myogenesis towards adipogenesis by inhibiting Rho GTPase in adipogenic precursor cells[17–19]. Another RhoGAP, DLC1, has been reported to promote both white and brown adipocyte differentiation and to provide a molecular link between PPARγ and Rho signaling pathways[20]. However, it's important to note that while p-190 B and DLC1 play significant roles in regulating adipocyte differentiation, neither of these RhoGAPs exhibits selective induction of brown adipocyte differentiation. In our current study, we present the unique contribution of GRAF1, a RhoGAP, to the differentiation of brown adipocytes. This distinctive function differentiates GRAF1 from other RhoGAPs. Combining in vitro investigations across various cell types with in vivo experiments in GRAF1 knockout mouse models, we have demonstrated that GRAF1 promotes classical brown fat maturation. This regulation, at least partly, occurs through GRAF1's ability to suppress RhoA activity, thereby limiting the RhoA-ROCK signal pathway and promoting brown adipocyte differentiation and maturation. Future research may elucidate the potential for manipulating GRAF1 expression and its GAP activity to improve metabolic profiles, holding promise for the treatment of metabolic diseases, including obesity and insulin resistance.

Methods

Animals

GRAF1 gene trap mice were generated and obtained from the Texas A&M Institute for Genomic Medicine (College Station, TX) and were described previously[30]. ES cells carrying Arhgap26 targeted knockout first conditional-ready alleles were obtained from EuMMCR. Germline transmission of the allele was confirmed from F0 chimeric mice with C57BL/6 genetic background. Next, we crossed Flp recombinase transgenic mice with F1 to generate GRAF1 floxed mice. Finally, we established adipose specific GRAF1 knockout mouse line (GRAF1^{AKO}) by crossing Adipoq-Cre line (010803, Jackson Lab[38]) with GRAF1 floxed mice. The GRAF1$^{flox/flox}$ mice were used as WT control. All mice were housed in pathogen-free facilities under a 12- hour light/dark cycle with unrestricted access to food and water. Animals were treated in accordance with the approved protocol of the University of North Carolina (Chapel Hill, NC) Institutional Animal Care and Use Committee, which is in compliance with the standards outlined in the guide for the Care and Use of Laboratory Animals. All methods are reported in accordance with ARRIVE (Animal Research: Reporting of In Vivo Experiments) guidelines.

Cold exposure

To assess sensitivity to cold exposure, we monitored rectal temperature at hourly intervals following the placement of female mice in a cold room maintained at 6–8 ℃. The mice underwent an overnight fast, which continued throughout the duration of the cold exposure. Subsequent to the cold exposure period, mice were humanely euthanized by CO_2 inhalation. To assess UCP1 expression and lactate levels in cold exposed animals, female mice were fed ad libitum prior to and throughout the cold challenge to aid in thermoregulation.

Cell culture and differentiation

Human Simpson-Golabi-Behmel syndrome (SGBS) preadipocyte line was provided by Dr. Martin Wabitsch (Ulm University Medical Center, Germany). The cells were maintained in DMEM/F12 (ThermoFisher Scientific,

11330-032) supplemented with 10% fetal calf serum(FCS), biotin 3.3 mM, pantothenate 1.7 mM and antibiotics. When cells were 90–100% confluence, SGBS cells were induced in brown adipocyte differentiation medium for 4 days (DMEM/F12, 3.3 mM biotin, 1.7 mM pantothenate, transferrin 10 µg/ml, 430 nMol insulin, 1nMol T3, 1µMol dexamethasone, 0.5mMol IBMX, 2µMol Rosiglitazone and antibiotics). Then cell medium was changed to brown adipocyte maintenance medium every 4 days for 8 days (DMEM/F12, 3.3 mM biotin, 1.7 mM pantothenate, transferrin 10 µg/ml, 430 nMol insulin, 1nMol T3 and antibiotics).

3T3-L1 cells were cultured in a six-well plate in growth media consisting of DMEM (ThermoFisher Scientific, 11965118) supplemented with 10% fetal calf serum (FCS) and penicillin-streptomycin (P/S). The cells were grown in DMEM until reaching 80% confluency, with medium changes every 2–3 days. Induction of 3T3-L1 browning was initiated using growth media supplemented with 10 µg/mL insulin, 1 µM dexamethasone, and 0.5 mM 3-isobutyl-1-methylxanthine (IBMX) for 2 days. From day 3 to day 8, cells were cultured in growth media supplemented with 10 µg/mL insulin, 1 µM dexamethasone, 0.5 mM IBMX, 1 µm Rosiglitazone and 50 nm triiodothyronine (T3).

WT-1 cells were provided by Dr. Yu-Hua Tseng (Joslin Diabetes Center, Harvard Medical School Affiliate, Boston, MA). WT-1 cells were maintained in DMEM (ThermoFisher Scientific, 11965118) supplemented with 10% fetal calf serum (FCS) and penicillin-streptomycin (P/S). To induce WT-1 differentiation, WT-1 cells were cultured in growth medium supplemented with 20 nM insulin and 1 nM T3 (differentiation medium). After reaching confluence, cells were cultured for 48 h in differentiation medium supplemented with 0.5 mM IBMX, 1 µm dexamethasone and 0.125 mM indomethacin. Subsequently, cells were cultured in differentiation medium for indicated days.

Isolation and differentiation of stromal vascular fraction (SVF) cells

Subcutaneous WAT (inguinal WAT) or inter-scapular BAT tissues were used for Beige cell source, and followed a previously described isolation and differentiation method[50]. In brief, tissues were digested and centrifuged to get SVF cells. SVF cells were cultured to 100% confluence in complete medium (DMEM/F12 containing 10% FCS and P/S). SVF cells were cultured for 2 days in induction medium (complete medium plus 5 µg/ml insulin, 1 nM T3, 125 µM Indomethacin, 2 µg/ml Dexamethasone, 0.5 mM IBMX, 0.5 µM Rosiglitazone). Then cell medium was changed to maintenance medium (complete medium plus 5 µg/ml insulin, 1 nM T3) with 0.5 µM Rosiglitazone for 2 days. At Day 4, cell medium was changed to maintenance medium with 1 µM Rosiglitazone for 2 days.

SiRNA treatment

Cells were plated in 6 well plate. Next day, cells were transfected GRAF1-targeting siRNA or GFP- targeting siRNA by Lipofectamine® RNAiMAX(ThermoFisher Scientific, 13778075) following the manufacturer's instructions. GRAF1 Stealth siRNA was synthesized by ThermoFisher with the following sequences: 5'-UCUUC ACUUUCUAUCACCAUGGUUA-3' and 5'- UAACCAUGGUGAUAGAAAGUGAAGA-3'. GFP stealth siRNA was used as Control with the following sequence: 5'-GGUGCGCUCCUGGACGUAGCC[dT][dT]-3'.

5'-GGCUACGUCCAGGAGCGCACC[dT][dT]-3'. Differentiation of WT-1 and SGBS started 24 h after siRNA treatment while differentiation of SVF cells started 72 h after treatment and GRAF1 levels remained reduced throughout the treatment regimen.

Real time qPCR analysis

Total RNA was isolated from homogenized whole mouse tissues or cell cultures using RNeasy Mini Kit (Qiagen, 74106) according to manufacturer's instructions. After homogenizing, samples were placed on ice to remove lipid layer. Complimentary DNA (cDNA) was obtained from 1 µg of RNA isolated using the iScript cDNA Synthesis Kit (Bio-Rad, 1708897), and cDNA was used for qRT-PCR with iTaq Universal SYBR Green Supermix kit (Bio-Rad, 1725124). The relative gene expression levels were calculated using delta-delta Ct method, also known as the 2–ΔΔCt method. Primer sequences were in Supplemental Table 1.

RhoA activity assay

WT-1 cells were serum starved overnight prior to treatment with sphingosine-1-phosphate (S1P) for indicated times. Rho activity was measured by GST-Rhotekin pulldown assay as previously described[51]. Cell lysates were rotated with 40 µg of a GST-rhotekin Rho binding domain fusion protein immobilized to glutathione-Sepharose 4B beads (Cytiva, 17075601) for 15 min at 4 °C in binding buffer (50 mM Tris, pH 7.6, 500 mM NaCl, 0.1% SDS, 0.5% deoxycholate, 1% Triton X-100, 0.5 mM MgCl2). Beads were precipitated and washed three times (50 mM Tris, pH 7.6, 150 mM NaCl, 1% Triton X-100, 0.5 mM MgCl2) and resuspended in 2 × Laemmli buffer. Proteins were separated on a 15% SDS–PAGE and transferred to 0.2 µm PVDF membrane (Bio-Rad, 1620177). After blocking in 5% bovine serum albumin/TBST (20 mM Tris–HCl, 500 mM NaCl, 0.05% Tween-20, pH 7.4) for 1 h at room temperature, blots were probed with 2 µg/ml anti-RhoA (26C4) (Santa Cruz Biotechnology, SC418) overnight at 4 °C. Loading controls (typically 10%) were taken from each lysate sample prior to pull downs.

Immunohistochemistry

Adipose tissue sections were deparaffinized, rehydrated, and washed prior to heat-induced antigen retrieval in citrate buffer. Sections were then washed, permeabilized, and protein blocked in goat serum and BSA prior to overnight incubation in UCP1 primary antibody (Cell Signaling Technology 14670) diluted 1:2000 in protein block buffer at 4 °C. Sections were then washed and peroxidase blocked in hydrogen peroxide prior to incubation in biotinylated rabbit secondary antibody (Jackson ImmunoResearch Laboratories, Inc. 111-065-144) diluted 1:500 in protein block buffer for 1 h at room temperature. Sections were then washed before incubation in VECTASTAIN Elite ABC reagent for 30 min. Sections were then washed and incubated in DAB Quanto reagent

at room temperature until sufficiently stained. Finally, sections were washed and mounted in Fluoromount-G before sealing the coverslips with nail polish. Micrographs were then obtained with an Olympus BX61 upright widefield microscope with brightfield with a 20X/0.75 UPlanSApo objective and a QImaging RETIGA 4000R camera, which is housed and maintained by the Microscopy Services Laboratory (UNC Chapel Hill).

Western blotting

To examine protein levels, lysates from cells or tissues were prepared by lysing in a modified RIPA buffer with 1x HALT phosphatase & protease inhibitor cocktail(ThermoFisher Scientific, 78438 and 78427). Protein concentration was determined by using a colorimetric BCA assay (Pierce, 23227). Lysates were electrophoresed on SDS–polyacrylamide gel, transferred to nitrocellulose and immunoblotted with specific antibodies overnight at 4℃ as indicated using a 1:1000 dilution. The following primary antibodies were used in western blot: GAPDH(cell signaling technology, 5174 S), b-actin(cell signaling technology, 3700 S), α-Tubulin(Sigma, T6199), RhoA(Santa Cruz, SC-418), UCP1(Abcam, ab10983). Rabbit anti-GRAF1 polyclonal antibody is homemade antibody in our lab. Blots were washed in TBST (TBS plus 0.1%Tween20) followed by incubation with horseradish peroxidase conjugated antibody at a 1/1,000 dilution. Blots were visualized after incubation with chemiluminescence reagents (ThermoFisher Scientific, 32106).

Oil red O staining and quantification

Cells were rinsed with PBS and then fixed in 4% PFA for 30 min. Then cells were left in the air until completely dry. Oil Red-O working solution (0.3%) was freshly prepared and stained cells on the shaker for 10 min. Then cells were rinsed with PBS 3 times and used for imaging. After imaging, liquid was removed from cells completely. To elute the oil red O dye, 100% isopropanol was added to the plates. The plates were incubated for 10 min at room temperature on an orbital shaker. Absorption was measured at 518 nm on a plate reader.

Statistics

Unless stated otherwise, all data represented at least three individual experiments and are presented as means ± standard error of the mean (SEM). Means of normally distributed data were compared by two-tailed Student's t-test, one-way ANOVA (followed by Tukey's post-hoc correction) or linear regression where indicated and statistical significance was reported as p-values. A p-value < 0.05 was considered significant. Sample sizes were chosen based on an extensive literature search. Definitive outliers as identified by the ROUT ($Q = 0.1\%$) method with GraphPad Prism were excluded from further analysis.

Data availability

All data generated or analyzed during this study are included in this published article and its supplementary information files.

Received: 11 December 2023; Accepted: 7 November 2024
Published online: 20 November 2024

References

1. Sanchez-Gurmaches, J. & Guertin, D. A. Adipocytes arise from multiple lineages that are heterogeneously and dynamically distributed. *Nat. Commun.* **5**, 4099 (2014).
2. Huang, P., Schulz, T. J., Beauvais, A., Tseng, Y. H. & Gussoni, E. Intramuscular adipogenesis is inhibited by myo-endothelial progenitors with functioning Bmpr1a signalling. *Nat. Commun.* **5**, 4063 (2014).
3. Ahmadian, M. et al. PPARγ signaling and metabolism: the good, the bad and the future. *Nat. Med.* **19**, 557–566 (2013).
4. Hu, E., Liang, P. & Spiegelman, B. M. AdipoQ is a novel adipose-specific gene dysregulated in obesity. *J. Biol. Chem.* **271**, 10697–10703 (1996).
5. Zhou, Z. et al. Cidea-deficient mice have lean phenotype and are resistant to obesity. *Nat. Genet.* **35**, 49–56 (2003).
6. Betz, M. J. & Enerback, S. Targeting thermogenesis in brown fat and muscle to treat obesity and metabolic disease. *Nat. Rev. Endocrinol.* **14**, 77–87 (2018).
7. Schulz, T. J. & Tseng, Y. H. Brown adipose tissue: development, metabolism and beyond. *Biochem. J.* **453**, 167–178 (2013).
8. Elsen, M. et al. BMP4 and BMP7 induce the white-to-brown transition of primary human adipose stem cells. *Am. J. Physiol. Cell. Physiol.* **306**, C431–C440 (2014).
9. Gustafson, B. et al. BMP4 and BMP antagonists regulate human white and Beige adipogenesis. *Diabetes* **64**, 1670–1681 (2015).
10. Tseng, Y. H. et al. New role of bone morphogenetic protein 7 in brown adipogenesis and energy expenditure. *Nature* **454**, 1000–1004 (2008).
11. Blázquez-Medela, A. M., Jumabay, M. & Boström, K. I. Beyond the bone: bone morphogenetic protein signaling in adipose tissue. *Obes. Rev. Official J. Int. Assoc. Study Obes.* **20**, 648–658 (2019).
12. Sharma, A. et al. Brown fat determination and development from muscle precursor cells by novel action of bone morphogenetic protein 6. *PLoS One* **9**, e92608 (2014).
13. Wei, L., Surma, M., Yang, Y., Tersey, S. & Shi, J. ROCK2 inhibition enhances the thermogenic program in white and brown fat tissue in mice. *Faseb j* **34**, 474–493 (2020).
14. Khan, A. U., Qu, R., Fan, T., Ouyang, J. & Dai, J. A glance on the role of actin in osteogenic and adipogenic differentiation of mesenchymal stem cells. *Stem Cell Res. Ther.* **11**, 283 (2020).
15. McDonald, M. E. et al. Myocardin-related transcription factor A regulates conversion of progenitors to beige adipocytes. *Cell* **160**, 105–118 (2015).
16. Rosenwald, M., Efthymiou, V., Opitz, L. & Wolfrum, C. SRF and MKL1 independently inhibit Brown Adipogenesis. *PLoS One* **12**, e0170643 (2017).
17. Inagaki, T., Sakai, J. & Kajimura, S. Transcriptional and epigenetic control of brown and beige adipose cell fate and function. *Nat. Rev. Mol. Cell. Biol.* **17**, 480–495 (2016).
18. Seale, P. et al. Beier DR and Spiegelman BM. PRDM16 controls a brown fat/skeletal muscle switch. *Nature* **454**, 961–967 (2008).
19. Yin, H. et al. MicroRNA-133 controls brown adipose determination in skeletal muscle satellite cells by targeting Prdm16. *Cell. Metab.* **17**, 210–224 (2013).
20. Sim, C. K. et al. Regulation of white and brown adipocyte differentiation by RhoGAP DLC1. *PLoS One* **12** e0174761. (2017).

21. Taylor, J. M., Macklem, M. M. & Parsons, J. T. Cytoskeletal changes induced by GRAF, the GTPase regulator associated with focal adhesion kinase, are mediated by Rho. *J. Cell. Sci.* **112** (Pt 2), 231–242. (1999).
22. Taylor, J. M., Hildebrand, J. D., Mack, C. P., Cox, M. E. & Parsons, J. T. Characterization of graf, the GTPase-activating protein for rho associated with focal adhesion kinase. Phosphorylation and possible regulation by mitogen-activated protein kinase. *J. Biol. Chem.* **273**, 8063–8070. (1998).
23. Doherty, J. T. et al. Skeletal muscle differentiation and fusion are regulated by the BAR-containing Rho-GTPase-activating protein (Rho-GAP), GRAF1. *J. Biol. Chem.* **286**, 25903–25921 (2011).
24. Sanchez-Gurmaches, J. et al. PTEN loss in the Myf5 lineage redistributes body fat and reveals subsets of white adipocytes that arise from Myf5 precursors. *Cell. Metab.* **16**, 348–362 (2012).
25. Gensch, N., Borchardt, T., Schneider, A., Riethmacher, D. & Braun, T. Different autonomous myogenic cell populations revealed by ablation of Myf5-expressing cells during mouse embryogenesis. *Development* **135**, 1597–1604 (2008).
26. Charrasse, S. et al. RhoA GTPase regulates M-cadherin activity and myoblast fusion. *Mol. Biol. Cell.* **17**, 749–759. (2006).
27. Iwasaki, K., Hayashi, K., Fujioka, T. & Sobue, K. Rho/Rho-associated kinase signal regulates myogenic differentiation via myocardin-related transcription factor-A/Smad-dependent transcription of the Id3 gene. *J. Biol. Chem.* **283**, 21230–21241. (2008).
28. Zhu, Q. et al. GRAF1 integrates PINK1-Parkin signaling and actin dynamics to mediate cardiac mitochondrial homeostasis. *Nat. Commun.* **14**, 8187 (2023).
29. Murholm, M. et al. Dynamic regulation of genes involved in mitochondrial DNA replication and transcription during mouse brown fat cell differentiation and recruitment. *PLoS One* **4**, e8458 (2009).
30. Lenhart, K. C. et al. GRAF1 promotes ferlin-dependent myoblast fusion. *Dev. Biol.* **393**, 298–311 (2014).
31. Giralt, M. et al. Ontogeny and perinatal modulation of gene expression in rat brown adipose tissue. Unaltered iodothyronine 5'-deiodinase activity is necessary for the response to environmental temperature at birth. *Eur. J. Biochem.* **193**, 297–302 (1990).
32. Wang, Q. A., Tao, C., Gupta, R. K. & Scherer, P. E. Tracking adipogenesis during white adipose tissue development, expansion and regeneration. *Nat. Med.* **19**, 1338–1344 (2013).
33. Kodde, A. et al. Maturation of white adipose tissue function in C57BL/6j mice from weaning to young adulthood. *Front. Physiol.* **10**, 836 (2019).
34. Liu, X. et al. Paradoxical resistance to diet-induced obesity in UCP1-deficient mice. *J. Clin. Invest.* **111**, 399–407. (2003).
35. Ellis, J. M. et al. Adipose acyl-CoA synthetase-1 directs fatty acids toward beta-oxidation and is required for cold thermogenesis. *Cell. Metab.* **12**, 53–64. (2010).
36. Hui, S. et al. Glucose feeds the TCA cycle via circulating lactate. *Nature* **551**, 115–118. (2017).
37. Dufau, J. et al. Rydén M and Langin D. In vitro and ex vivo models of adipocytes. *Am. J. Physiol. Cell. Physiol.* **320**, C822–C841 (2021).
38. Eguchi, J. et al. Transcriptional control of adipose lipid handling by IRF4. *Cell. Metab.* **13**, 249–259 (2011).
39. Richard, A. J., White, U., Elks, C. M. & Stephens, J. M. Adipose Tissue: Physiology to Metabolic Dysfunction. In: K. R. Feingold, B. Anawalt, M. R. Blackman, A. Boyce, G. Chrousos, E. Corpas, W. W. de Herder, K. Dhatariya, K. Dungan, J. Hofland, S. Kalra, G. Kaltsas, N. Kapoor, C. Koch, P. Kopp, M. Korbonits, C. S. Kovacs, W. Kuohung, B. Laferrère, M. Levy, E. A. McGee, R. McLachlan, M. New, J. Purnell, R. Sahay, A. S. Shah, F. Singer, M. A. Sperling, C. A. Stratakis, D. L. Trence and D. P. Wilson, (ed) *Endotext* South Dartmouth (MA): MDText.com, Inc. Copyright © 2000–2023, MDText.com, Inc. (2000).
40. Sakers, A., De Siqueira, M. K., Seale, P. & Villanueva, C. J. Adipose-tissue plasticity in health and disease. *Cell* **185**, 419–446 (2022).
41. Harms, M. J. et al. Prdm16 is required for the maintenance of brown adipocyte identity and function in adult mice. *Cell. Metab.* **19**, 593–604. (2014).
42. Liu, P. et al. Foxp1 controls brown/beige adipocyte differentiation and thermogenesis through regulating β3-AR desensitization. *Nat. Commun.* **10**, 5070 (2019).
43. Liang, H. & Ward, W. F. PGC-1alpha: a key regulator of energy metabolism. *Adv. Physiol. Educ.* **30**, 145–151 (2006).
44. Cristancho, A. G. & Lazar, M. A. Forming functional fat: a growing understanding of adipocyte differentiation. *Nat. Rev. Mol. Cell. Biol.* **12**, 722–734. (2011).
45. Etienne-Manneville, S. & Hall, A. Rho GTPases in cell biology. *Nature* **420**, 629–635. (2002).
46. Klepac, K. et al. Insel PA and Pfeifer A. The Gq signalling pathway inhibits brown and beige adipose tissue. *Nat. Commun.* **7**, 10895 (2016).
47. Lucken-Ardjomande Häsler, S., Vallis, Y. & Jolin, H. E. McKenzie AN and McMahon HT. GRAF1a is a brain-specific protein that promotes lipid droplet clustering and growth, and is enriched at lipid droplet junctions. *J. Cell. Sci.* **127**, 4602–4619 (2014).
48. Lundmark, R. et al. The GTPase-activating protein GRAF1 regulates the CLIC/GEEC endocytic pathway. *Curr. Biol. CB* **18**, 1802–1808. (2008).
49. Chow, L. S. et al. Goodpaster BH and Snyder MP. Exerkines in health, resilience and disease. *Nat. Rev. Endocrinol.* **18**, 273–289. (2022).
50. Aune, U. L., Ruiz, L. & Kajimura, S. Isolation and differentiation of stromal vascular cells to beige/brite cells. *J. Visualized Exp. JoVE* (2013).
51. Bai, X. et al. The smooth muscle-selective RhoGAP GRAF3 is a critical regulator of vascular tone and hypertension. *Nat. Commun.* **4**, 2910. (2013).

Acknowledgements

We thank Kent Murley for aiding in the construction the figures for this manuscript. This research is based in part upon work conducted at the Microscopy Services Laboratory, Department of Pathology and Laboratory Medicine, which are supported in part by a National Cancer Institute Cancer Center Core Support Grant to the University of North Carolina Lineberger Comprehensive Cancer Center (P30 CA016086). This work was also supported by NIH including NHLBI/R01HL130367 and 1RO1HL165786 to JMT, 1F31HL145983-01 to M.E.C., and American Heart Association 16PRE30630002 to Q.Z. and a North Carolina Obesity Research Center Pilot Award to XB.

Author contributions

Conceived and performed experiments, data analysis and preliminary manuscript writing: XB. Conceived and performed experiments, data analysis and final manuscript writing: QZ. Conceived and performed experiments and data analysis: MEC. Development of SBGS cell line, distribution and guidance of usage: MW. Conceptual development of studies and manuscript preparation: CPM. Conceptual development of studies and manuscript preparation: JMT.

Declarations

Competing interests
The authors declare no competing interests.

Additional information
Supplementary Information The online version contains supplementary material available at https://doi.org/10.1038/s41598-024-79301-6.

Correspondence and requests for materials should be addressed to J.M.T.

Reprints and permissions information is available at www.nature.com/reprints.

Publisher's note Springer Nature remains neutral with regard to jurisdictional claims in published maps and institutional affiliations.